Conf-720522--2

MASTER

REMOVAL OF URANIUM FROM MOLTEN FLUORIDE MIXTURES*

J. R. Hightower, Jr. B. A. Hannaford
M. J. Bell L. E. McNeese

NOTICE

This report was prepared as an account of work sponsored by the United States Government. Neither the United States nor the United States Atomic Energy Commission, nor any of their employees, nor any of their contractors, subcontractors, or their employees, makes any warranty, express or implied, or assumes any legal liability or responsibility for the accuracy, completeness or usefulness of any information, apparatus, product or process disclosed, or represents that its use would not infringe privately owned rights.

Oak Ridge National Laboratory
P. O. Box X
Oak Ridge, Tennessee 37830

*Research sponsored by the U. S. Atomic Energy Commission under contract with the Union Carbide Corporation.

DISTRIBUTION OF THIS DOCUMENT IS UNLIMITED

REMOVAL OF URANIUM FROM MOLTEN FLUORIDE MIXTURES

J. R. Hightower, Jr. B. A. Hannaford
M. J. Bell L. E. McNeese

1. INTRODUCTION

The MSBR is fueled with a molten mixture of LiF, BeF_2, and ThF_4 in which $^{233}UF_4$ is dissolved. The reference flowsheet for the processing plant calls for continuously removing the uranium from the molten fluoride mixture by fluorination before extraction of Pa and the rare earth fission products. In the fluorination step fluorine would be bubbled through the molten salt from the reactor to convert the nonvolatile UF_4 to volatile UF_6 which would be removed in the fluorinator off-gas.

Another flowsheet which is being examined calls for removal of uranium from the fluoride salt by precipitation as UO_2. In this process a gaseous mixture of water and argon is bubbled through the salt converting UF_4 to UO_2, a comparatively insoluble material, which precipitates as a UO_2-ThO_2 solid solution.

The purpose of this paper is threefold: (1) to describe our conception of a continuous fluorinator, (2) to describe our work on fluorinator development, and (3) to briefly describe results of small-scale uranium oxide precipitation experiments.

2. CONCEPTION OF CONTINUOUS FLUORINATOR

A conceptual drawing of a continuous fluorinator is shown in Fig. 1. The fluorinator is an open bubble column through which fluorine and molten salt flow

countercurrent to each other. The special feature of this piece of equipment is the means for protecting against corrosion by fluorine. The vessel itself will be made of nickel, which, in the absence of molten salts, exhibits satisfactory resistance to fluorine attack. This resistance results from a passivating film of NiF_2 corrosion product. However, when the molten salts are present, the NiF_2 is dissolved, leaving the metal substrate unprotected. We propose to keep the NiF_2 film on the vessel walls by covering the walls with a layer of frozen salt.

In order to maintain the salt frozen near the wall while the inner core is molten an internal heat source is necessary to support the temperature gradient. The requisite heat will be supplied in the MSBR processing plant by fission product decay. Heat generation rates in the molten salt will be up to 12.6 kW/ft^3.

The gas inlet must also be protected against corrosion, which precludes the use of an efficient gas distributor. Presently, large diameter, angled side entrances are being planned.

3. DEVELOPMENT FOR CONTINUOUS FLUORINATORS

Development of continuous fluorinators has been divided into four separate areas which will be discussed. These areas are (1) measurement and correlation of axial dispersion in open bubble columns, (2) measurement of basic rate constants for the fluorination reaction, (3) studies of frozen film formation for corrosion protection, and (4) methods for simulating heat generation in molten salts caused by the decay of fission products.

3.1 Axial Mixing in Open Bubble Columns

The successful operation of a fluorinator depends upon the establishment of a significant axial concentration gradient of dissolved uranium fluoride in the salt. It is important to be able to predict the effects of axial mixing caused by rising gas bubbles in the column, since mixing adversely affects the fluorinator

performance by flattening the concentration gradient, thereby lowering the fraction of uranium removed for a given fluorinator volume.

Because of difficulties associated with direct measurements of axial dispersion in molten salt systems, a comprehensive study of bubble-produced longitudinal dispersion was undertaken using air and aqueous solutions. The study was carried out using a range of conditions in order to be able to extrapolate to molten salt systems. A model for correlating the data was chosen in which mixing is quantized in terms of an effective longitudinal diffusivity or dispersion coefficient that is defined by the one-dimensional diffusion equation. The effects of column diameter, liquid physical properties, gas distributor design and gas flow rate were determined and a generalized correlation of these effects was developed.

Gas holdup and axial dispersion were determined by both steady state and transient techniques by measuring concentration profiles of a dye or an electrolyte tracer in columns having diameters ranging from 1 to 6 in. Glycerol-water solutions, with viscosities ranging from 0.9 to 12 cP, and aqueous isobutanol or isopropanol solutions whose surface tensions varied from 72-27 dyne/cm were used. Superficial air velocities were varied up to about 40 cm/sec (79 ft/min). The gas distributor was either a single orifice or a plate with 5 gas inlets. Two flow regimes were noted. At low superficial gas velocities, the bubbles rose as discrete entities and no coalescence was observed. At high superficial gas velocities, the bubbles coalesced into large bubbles whose diameter was essentially equal to the column diameter. The axial dispersion coefficient was found to follow a power law dependence on the superficial gas velocity as shown in Fig. 2. The exponent is 0.12 in the bubbly region and 0.6 in the slug flow region.

The dispersion was found to increase with increasing column diameter, increasing surface tension, and decreasing liquid viscosity. The dispersion increased with in-

creasing orifice diameter in bubbly flow, but it was independent of orifice diameter in slug flow.

A dimensional analysis identified the dimensionless groups pertinent to a quantitative description of dispersion, and a correlation between these groups was developed. Different correlations were found for bubble and for slug flow conditions. The correlation for bubble flow is shown in Fig. 3. The correlation expresses a Peclet number which contains the dispersion coefficient, the superficial gas velocity and the column diameter, as a power function of a Reynolds number, an Archimedes number, a Suratman number, and the number of orifices in the gas distributor.

Figure 4 shows the correlation for slug flow. Here the Peclet number is proportional to the Reynolds number to the 0.4 power, the Archimedes number to the 0.11 power, and the Suratman number to -0.38 power. In slug flow there was no influence of number of orifices.

The correlating velocity is the superficial gas velocity and the correlating length is the column diameter. The Reynolds numbers account for gas velocity effects; the Archimedes number, for buoyancy effects; and the Suratman number, for surface tension effects.

3.2 Measurements of Uranium Removal in a 1-in.-OD Bubble Column

Experimental studies of continuous fluorination of molten salt have been made in a 1-in.-diam, 72-in.-long nickel fluorinator which allowed countercurrent contact of molten salt with F_2. The equipment is shown in Fig. 5.

The fluorinator was made of 1 in. sched 40 nickel pipe with a salt depth of 48 in. The off-gas passed through a 400°C NaF bed for removal of chromium fluorides, a 100°C NaF bed for removal of UF_6, and a soda lime bed for F_2 disposal. A gas chromatograph was used to analyze the off-gas for F_2, UF_6, and N_2 just prior to the 100°C NaF trap. The uranium concentration in the salt after fluorination was determined from salt samples.

In these fluorination tests, molten salt (41-25-35 mole % $NaF-LiF-ZrF_4$) containing UF_4 was contacted countercurrently with a quantity of F_2 in excess of that required for conversion of the UF_4 to UF_6. During a given experiment, salt and fluorine feed rates, operating temperature, and UF_4 concentration in the feed salt remained constant. All the experiments covered the following range of the parameters: operating temperature ranged from 525 to 600°C; salt feed rate, ranged from 5 to 30 cm^3/min; fluorine feed rates ranged from 215 to 410 cm^3/min; and UF_4 concentration in the feed salt ranged from 0.12 to 0.35 mole % UF_4.

The results of the fluorination experiments are shown in Fig. 6. The data are based on the concentration of uranium remaining in the fluorinated salt. The uranium remaining in the salt increased as the salt throughput increased, as the operating temperature was lowered, and as the concentration in the feed salt was decreased. As long as the quantity of fluorine was stoichiometrically adequate, no significant effect of fluorine feed rate was noticed.

The equations for chemical reaction in a tubular reactor with dispersion were used to evaluate a rate constant for the fluorination reaction assuming that the reaction was first order with respect to the uranium concentration in the liquid. Given the experimental gas flow rates, liquid properties and column dimensions, the dispersion coefficient in each experiment was evaluated from the correlation previously described. These dispersion coefficients were used in conjunction with the uranium removal data taken at 525°C to evaluate the rate constant. This rate constant was used, along with the dispersion correlation, in estimating the size of fluorinators needed for processing MSBRs.

The reference flowsheet calls for fluorination of fuel salt at the rate of 170 ft^3/day. A 6-in.-diam fluorinator having a height of 10.2 ft will be required for a uranium removal efficiency of 95% and an 8-in.-diam fluorinator having a height of 17.8 ft will be required for a uranium removal efficiency of 99%.

3.3 Frozen Film Formation

The feasibility of maintaining frozen films in a gas-salt contactor has been demonstrated. Figure 7 shows a diagram of equipment used for forming frozen salt on the wall of a gas-salt contactor. The test vessel was a 5-in.-diam, 8-ft-high column fabricated from sched 40 Ni pipe. The internal heat source consisted of 3 Calrod heaters contained in a 3/4-in. Ni pipe at the centerline of the test vessel. The salt was 66-34 mole % $LiF-ZrF_4$ which has a liquidus of 595°C. Argon was fed countercurrent to the salt in the system.

Frozen wall thicknesses were inferred from temperature readings from sets of thermocouples protruding various distances into the vessel from the wall. These thicknesses were confirmed in selected experiments by radiographs made after quickly draining the column and leaving the frozen wall in place. After the final experiment, the vessel was sectioned in order to examine the frozen film. A photograph of a section of the column is shown in Fig. 8. It can be seen that the salt film was in fact uniform and symmetrical. The actual film was the lighter material; the darker layer froze during draining after the last experiment.

The experiments were performed at equivalent volumetric heating rates of 10 to 55 kW/ft^3 which is higher than the heat generation in 1-day cooled salt from a reactor operating at steady state.

The inclined pipe fluorine inlet was found to be workable.

3.4 Internal Heat Source Development

Further studies of continuous fluorination in a system that uses frozen wall corrosion protection are planned using a salt which contains no radioactive fission

products. For this experiment, means for generating heat in the molten salt is required; the device for generating heat should not be subject to corrosion by the combined action of fluorine and molten salt. We have considered two methods for internal heat generation. These consist of radio-frequency induction heating and autoresistance heating with 60 Hz power. Details of these methods are shown schematically in Fig. 9.

With the induction heating method, an induction coil is imbedded in frozen salt which electrically insulates the coil from the vessel wall and from the molten salt. Electrical leads pass through the top of the vessel in such a manner that neither the coil nor the leads contact both fluorine and molten salt.

With the autoresistance heating method, an electrode contacts the molten salt in a side arm near the top of the fluorinating section. The lower part of the vessel is the other electrode and an electrically insulating salt film must be present to cause the heating current to pass along the section in which the fluorination reaction will be carried out.

A study of high frequency induction heating using nitric acid solutions in fluorinator simulations indicated that sufficient heat could be generated in the molten salt. However, the required generator, transmission lines, and power controls are complex; and it was found that there is a relatively narrow range of acceptable operating conditions.

Preliminary tests of autoresistance heating in a vessel with no side arm have been partially successful and autoresistance heating at the desired rates has been observed. The formation of an electrically insulating frozen salt layer has been more difficult than had been initially expected. However, it is believed that a method can be developed for reliably forming a frozen layer that is electrically insulating. Since power supplies for autoresistance heating are simpler and more flexible than ones for induction heating, a wider range of acceptable operating conditions is available and autoresistance heating is the preferred heating method.

After additional studies of autoresistance heating have been completed, we will design and build a continuous fluorinator that will operate with a molten zone diameter of about 5 in. and a height of about 5 ft.

4. EXPERIMENTS ON URANIUM REMOVAL BY OXIDE PRECIPITATION

Oxide precipitation is being considered for removing uranium and isolating protactinium from the fuel salt of MSBRs because it would be less demanding on materials of construction than would be a plant that uses fluorination.

The chemistry of separating uranium from the fuel salt by oxide precipitation appears favorable. Baes and Bamberger, of the Reactor Chemistry Division of ORNL, have measured the equilibrium between UO_2-ThO_2 solid solutions and molten fluoride salts. This data is shown in Fig. 10. With UF_4 compositions in the salt in the range found in the fuel salt, the UO_2-ThO_2 solid solution in equilibrium with the salt is about 95% UO_2. The fraction of UO_2 in the solid solution drops off sharply as the UF_4 concentration decreases below 0.1%. In order to reach fuel salt compositions of 30 ppm UF_4, this data shows that large quantities of ThO_2 must be precipitated with the UO_2 if precipitation is carried out in a single equilibrium precipitation stage. However, if a multistage equilibrium precipitator is used, calculations have shown that greater than 99% of the uranium can be precipitated as a solid solution containing less than 10% ThO_2 using only 3 to 4 equilibrium stages.

Initial engineering studies of precipitation of UO_2-ThO_2 solid solutions from MSBR fuel salts have been carried out in a single-stage precipitation facility. The purpose of these experiments were:

(1) to measure the effects of temperature and reactant feed rates on precipitation rate,

(2) to measure the composition of the UO_2-ThO_2 solid solutions formed under the nonequilibrium conditions,

(3) to gain experience with separating salt and oxide phases, and with gas-liquid-solid contacting during precipitation and hydrofluorination.

The basic components of the system are shown in Fig. 11. The facility consists of:

(1) a nickel precipitator vessel,

(2) an argon-steam gas mixture which was the source of oxide,

(3) a source of HF to convert oxide back to fluoride, and

(4) an HF collection and disposal system for treating off-gas from precipitation and hydrofluorination operations.

The operating sequence was as follows: Salt in the precipitator vessel was ontacted with an argon-water mixture in a draft tube to precipitate UO_2-ThO_2 olid solutions. and the progress of the reaction is followed by collecting nd measuring the HF evolved. When a sufficient amount of oxide had been pre-ipitated, the precipitate was allowed to settle for about 1 hr, after which amples of oxide and filtered salt samples were taken. After sampling, salt was lowly decanted by pressurizing the precipitator vessel with argon. The salt in he receiver was then hydrofluorinated to convert to fluoride any oxide which ight have been transferred, then the salt was sampled. The salt was then re-urned to the precipitator vessel, and the salt and oxide were hydrofluorinated convert the oxides to fluorides in preparation for the next experiment.

Results of oxide sample analyses obtained through the first 8 runs are nown in Fig. 12. The ratio of ThO_2 to UO_2 in these oxide samples are given as function of the uranium concentration in the salt. The data are plotted along ith values predicted by the equilibrium equation, which predicts that at low F_4 concentrations in the salt, the ratio of ThO_2 to UO_2 becomes quite large.

At high UF_4 concentrations, the data points agree fairly closely with the equilibrium calculation but fall well below the equilibrium curve at low uranium concentrations. These results have indicated that UO_2-ThO_2 solid solutions are precipitated at equilibrium with the UF_4 concentration in the salt at the moment of formation; but the solid solutions, once formed, do not rapidly re-equilibrate with the remaining salt which has progressively lower UF_4 concentrations. Thus, solid solutions which are formed early in the precipitation process, containing 90-95% UO_2, are still present in the final stages of precipitation, when the solid solutions being formed contain much less UO_2. A curve which represents thi model of the precipitation process is also shown in the figure. Based on this model, 99% of the uranium could be precipitated from the salt in <u>one</u> stage as a solid which contained 85% UO_2. It is believed that the experimental data actually fall between the two curves because inadequate mixing in the salt phase causes precipitation of a thorium-rich phase. The observed uranium content of the solid solutions are still well within the range of that required for a flowsheet using a single stage UO_2 precipitator.

Experiments were carried out in the temperature range of 540-630°C. Only a slight increase of reaction rate with temperature was observed, but the rate of precipitation appeared to vary in direct proportion to the rate at which water was supplied to the system. The precipitates were observed to settle rapidly and the salt was separated from the solids by decantation with little entrainment.

These experiments show that oxide precipitation appears to be an attractive alternative to fluorination for removing uranium from fuel salt from which the protactinium has been previously removed.

REFERENCES

Axial Dispersion and Fluorinator Performance

M. S. Bautista, L. E. McNeese, J. S. Watson, J. T. Day, and P. H. Wadia, "Axial Mixing in Open Bubble Columns," to be published.

D. E. Ferguson, Chem. Technol. Div. Annu. Rep. May 31, 1972, USAEC Rep., ORNL-4794, in preparation.

J. S. Watson and L. E. McNeese, "Predicted Performance of Continuous Fluorinators," MSR Program Semiannu. Prog. Rep. Aug. 31, 1971, USAEC Rep., ORNL-4728, p. 217.

Measurements of Uranium Removal

D. E. Ferguson, "Continuous Fluorination of Molten Fluoride Mixtures in 1-in.-diam Columns," Chem. Technol. Div. Annu. Progr. Rep. May 31, 1967, USAEC Rep., ORNL-4145, p. 95.

Frozen Film Formation

B. A. Hannaford and L. E. McNeese, "Continuous Fluorination of Molten Salt," MSR Program Semiannu. Progr Rep. Feb. 29, 1968, USAEC Rep., ORNL-4254, p. 252.

B. A. Hannaford and L. E. McNeese, "Continuous Fluorination of Molten Salt," MSR Program Semiannu. Progr. Rep. Aug. 31, 1968, USAEC Rep., ORNL-4344, p. 302.

Internal Heat Source Development

J. R. Hightower, Jr. and C. P. Tung, "Development of a Frozen-Wall Fluorinator," MSR Program Semiannu. Progr. Rep. Feb. 28, 1971, USAEC Rep., ORNL-4676, p. 262.

J. R. Hightower, Jr., "Development of a Frozen-Wall Fluorinator: Induction Heating Experiments," MSR Program Semiannu. Prog. Rep. Aug. 31, 1971, USAEC Rep., ORNL-4728, p. 214.

J. R. Hightower, Jr., "Frozen-Wall Fluorinator Development," MSR Program Semiannu. Progr. Rep. Feb. 29, 1972, USAEC Rep., ORNL-4728, in preparation.

REFERENCES (Continued)

Uranium Removal by Oxide Precipitation

M. J. Bell, D. D. Sood, and L. E. McNeese, "Engineering Studies of Uranium Removal by Oxide Precipitation," MSR Program Semiannu. Progr. Rep. for Aug. 31, 1971, USAEC Rep., ORNL-4728, p. 220.

M. J. Bell and L. E. McNeese, "Engineering Studies of Uranium Removal by Oxide Precipitation," MSR Program Semiannu. Progr. Rep. for Feb. 28, 1971, USAEC Rep., ORNL-4676, p. 267.

C. E. Bamberger and C. F. Baes, Jr., J. Nucl. Matl. 35, 177 (1970).

ORNL DWG 72-1438

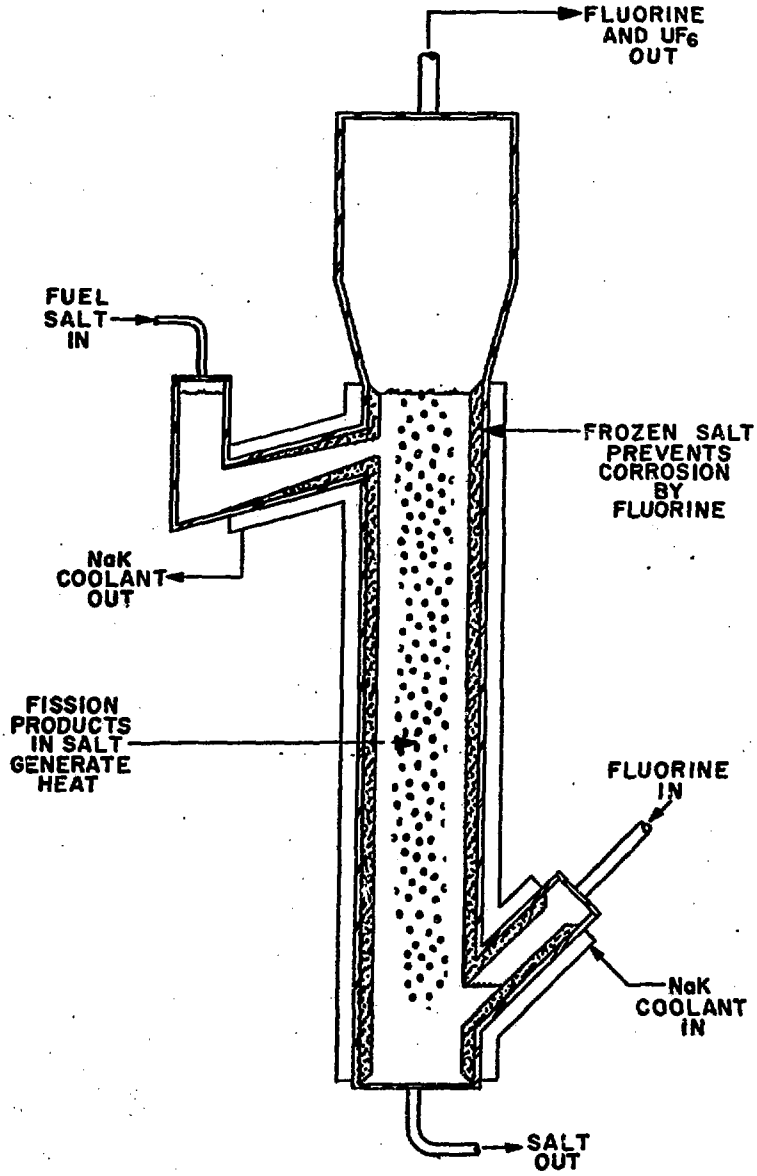

Fig. 1. Continuous Fluorinator with Frozen Salt Wall for Corrosion Protection.

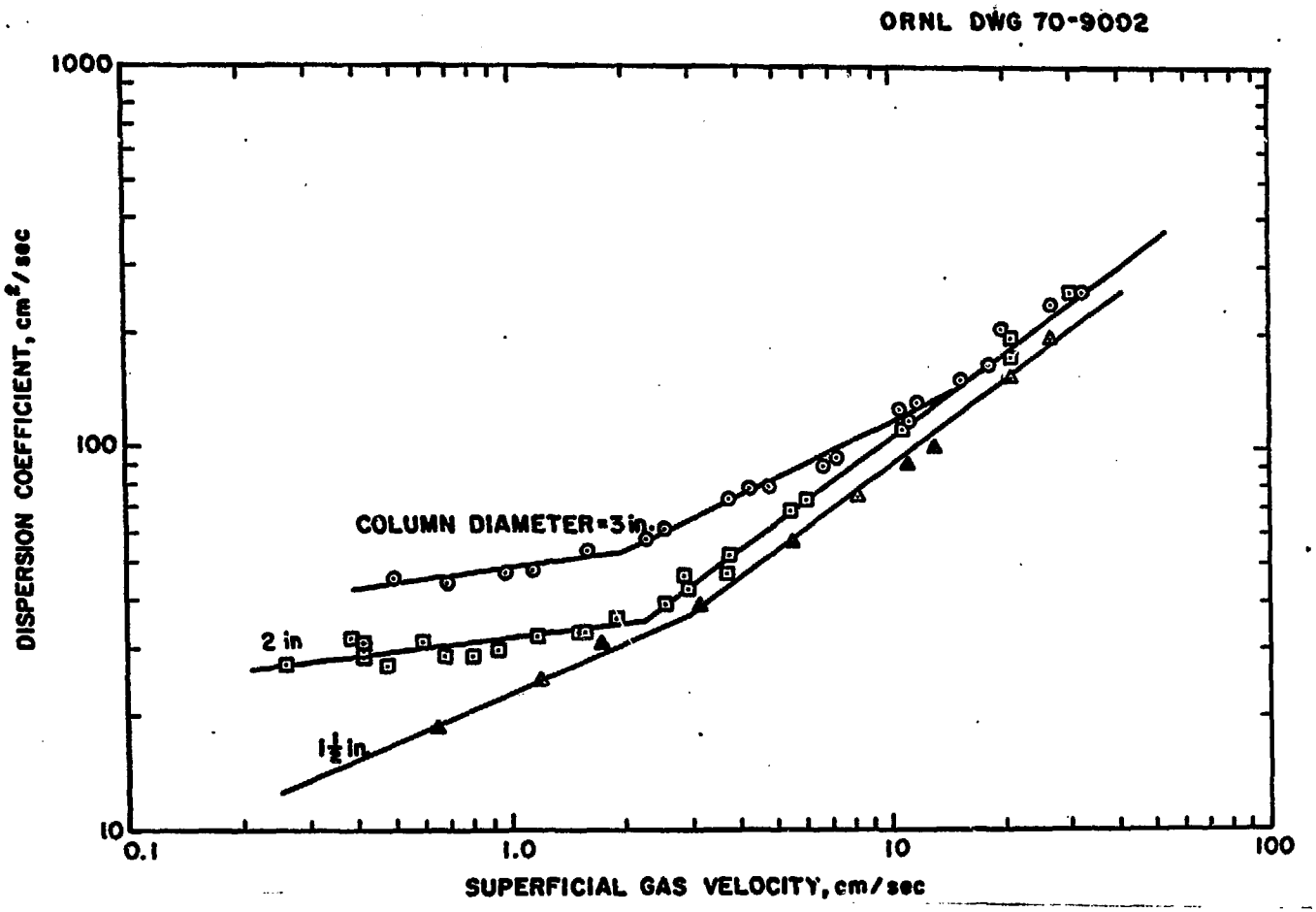

Fig. 2. Variation of Dispersion Coefficient with Superficial Gas Velocity and Column Diameter in Open Bubble Columns.

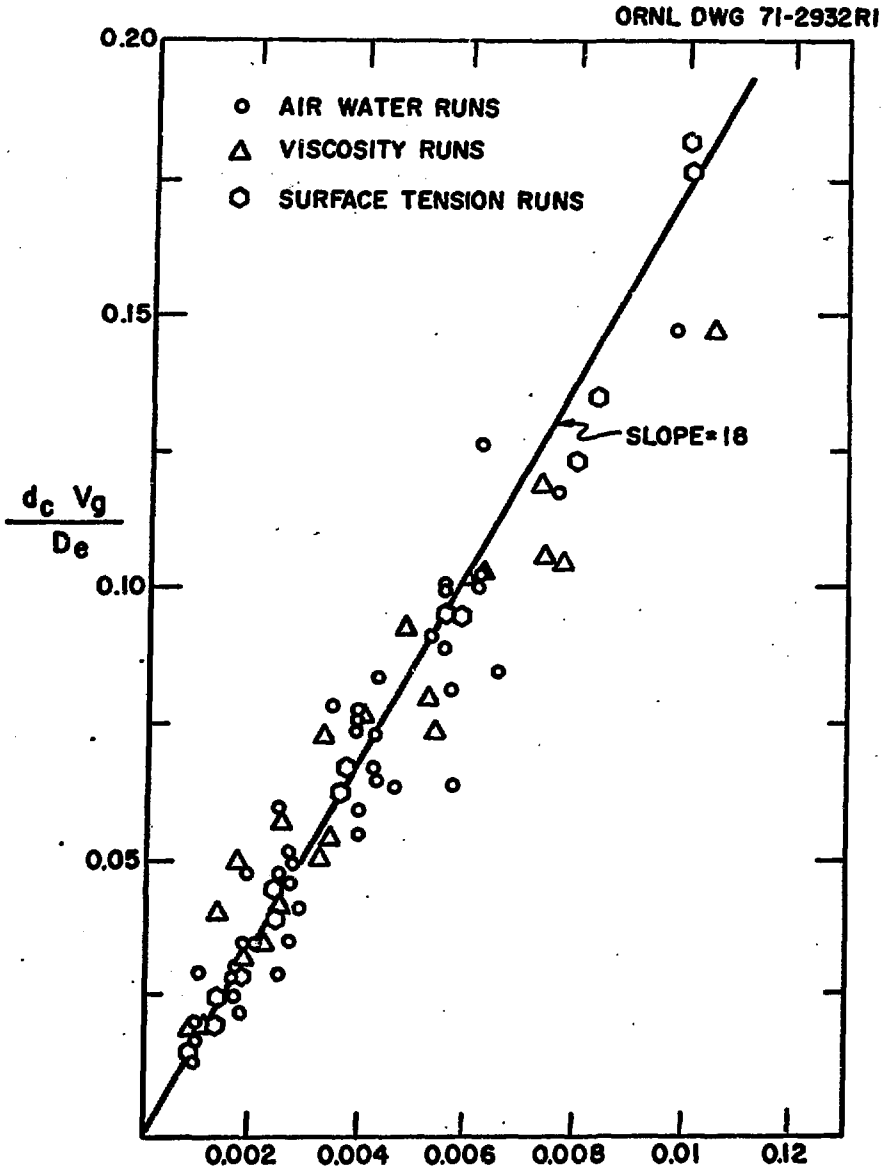

$$\left(\frac{\rho_l d_c V_g}{\mu_l}\right)^{0.88}\left(\frac{d_c^3 \rho_l^2 g}{\mu_l^2}\right)^{-0.435}\left(\frac{d_c \rho_l \sigma}{\mu_l}\right)^{-0.075} N^{-0.0475}$$

Fig. 3. Correlation of Dispersion Coefficient In Open Bubble Columns for Bubbly Flow Conditions.

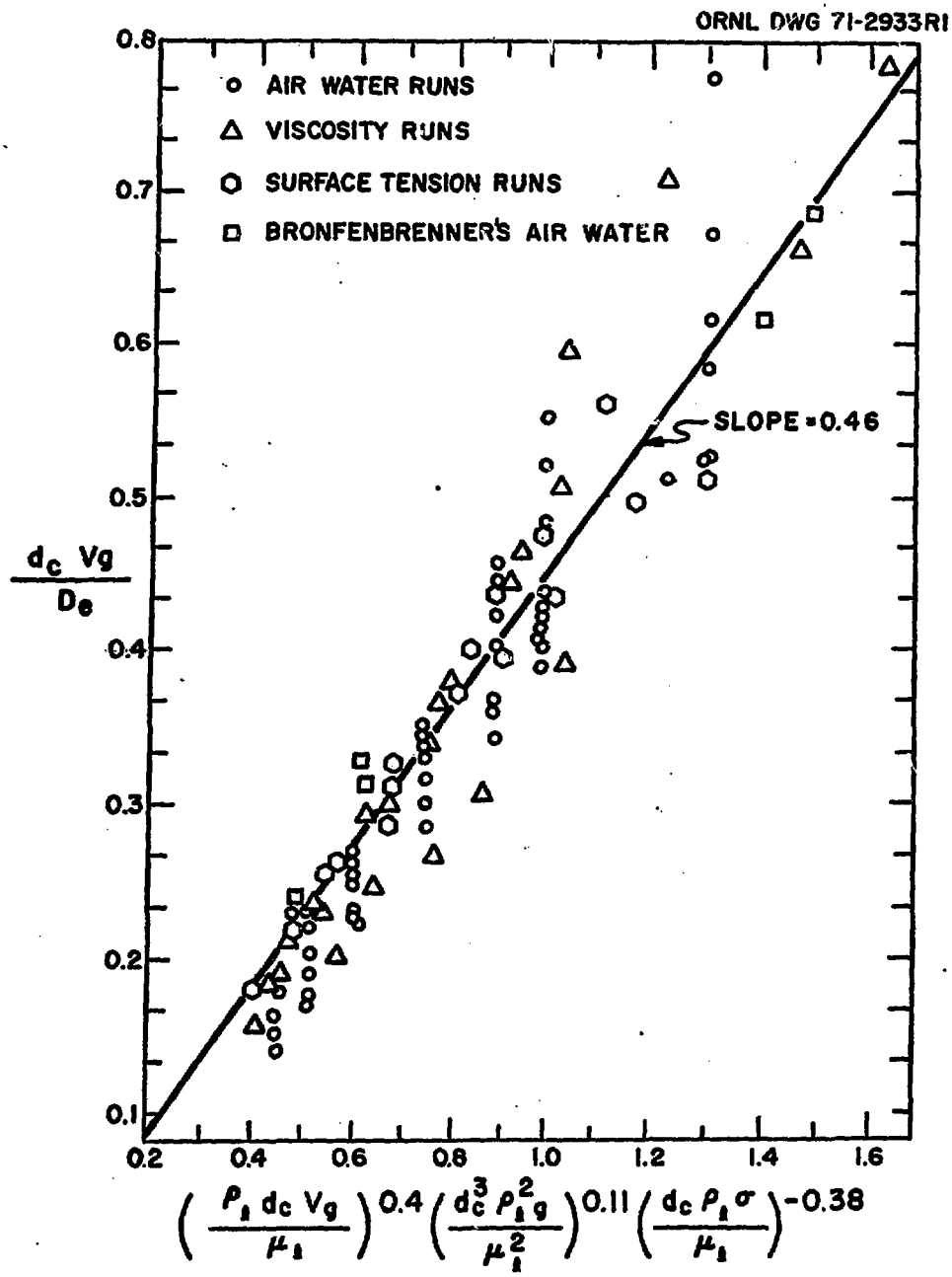

Fig. 4. Correlation of Dispersion Coefficient In Open Bubble Columns for Slug Flow Conditions.

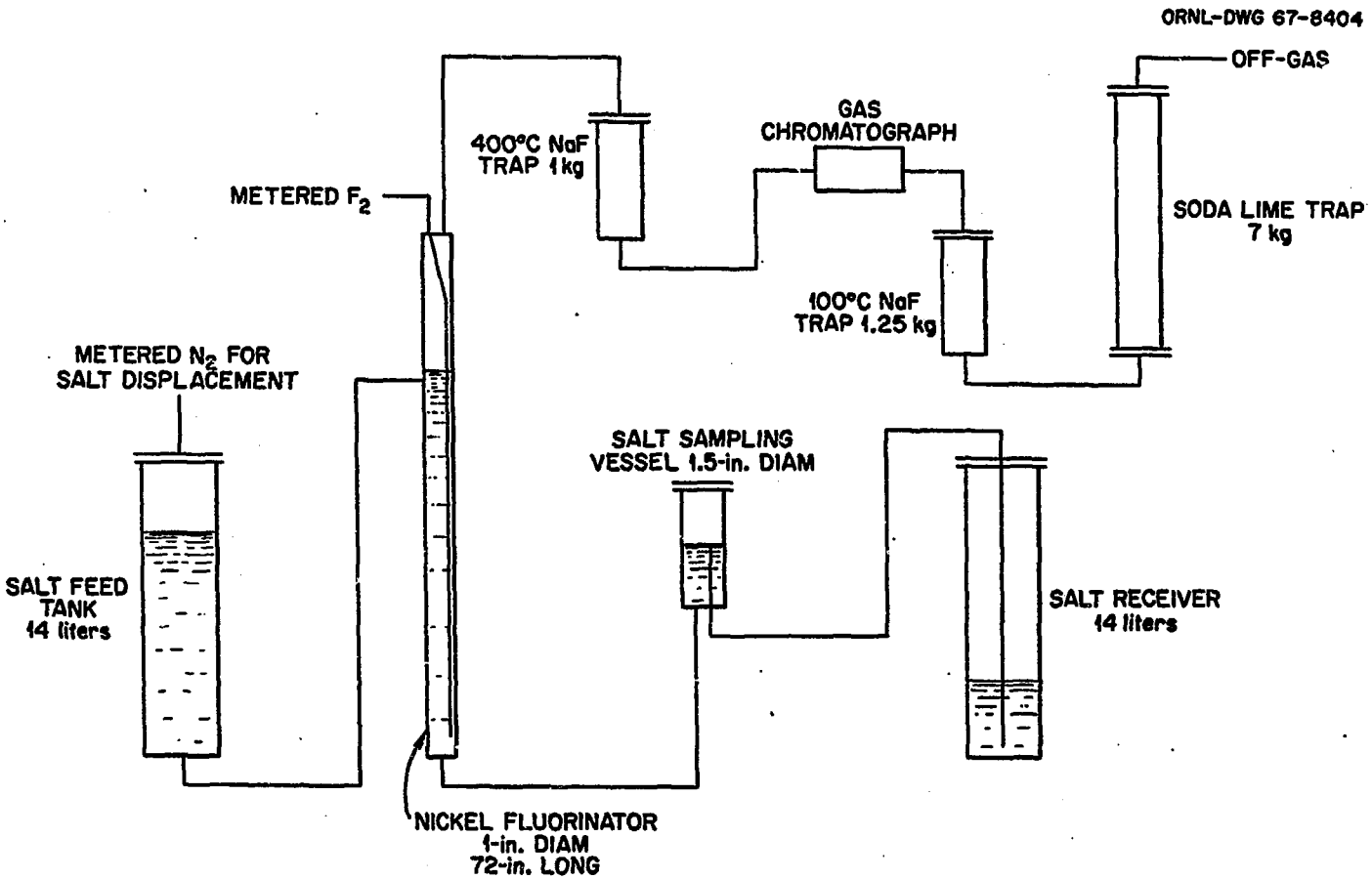

Fig. 5. Flow Diagram of Equipment for Removal of Uranium from Molten Salt by Continuous Fluorination.

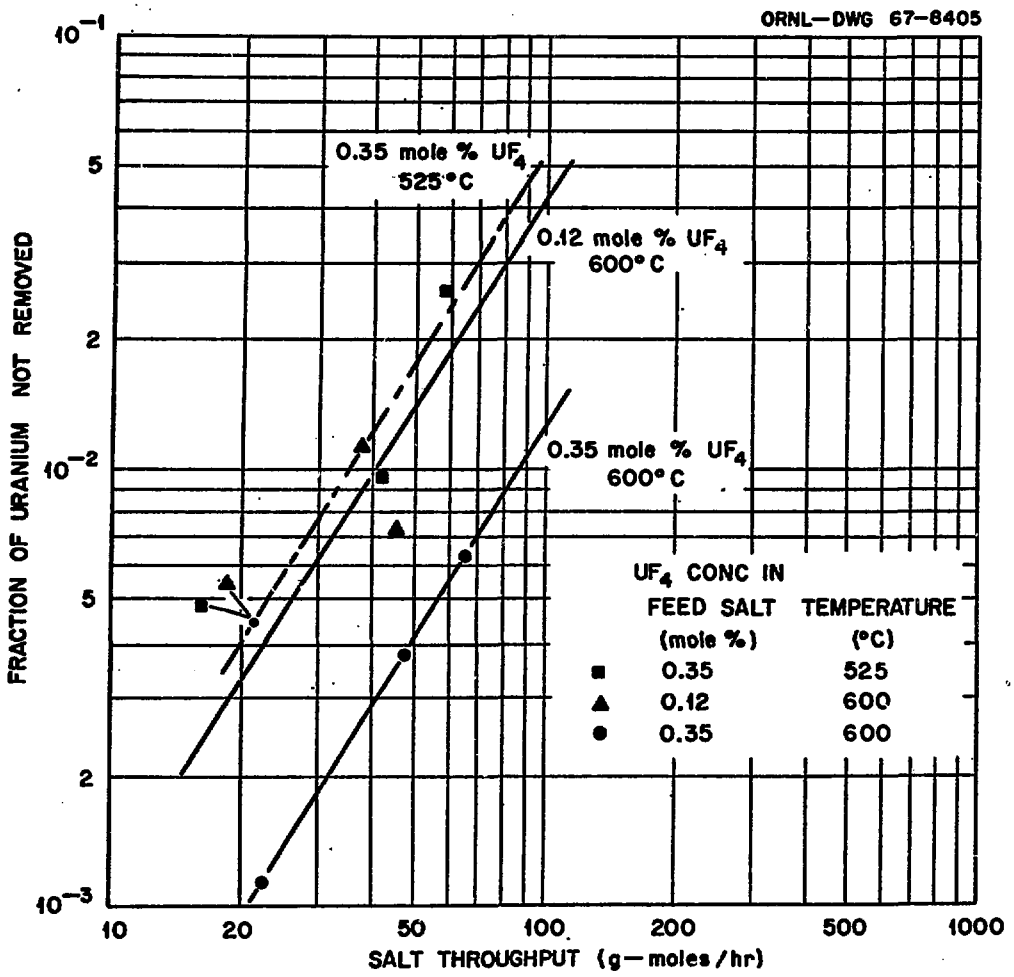

Fig. 6. Variation of Uranium Removal with Salt Throughput, Operating Temperature, and UF_4 Concentration in Feed Salt.

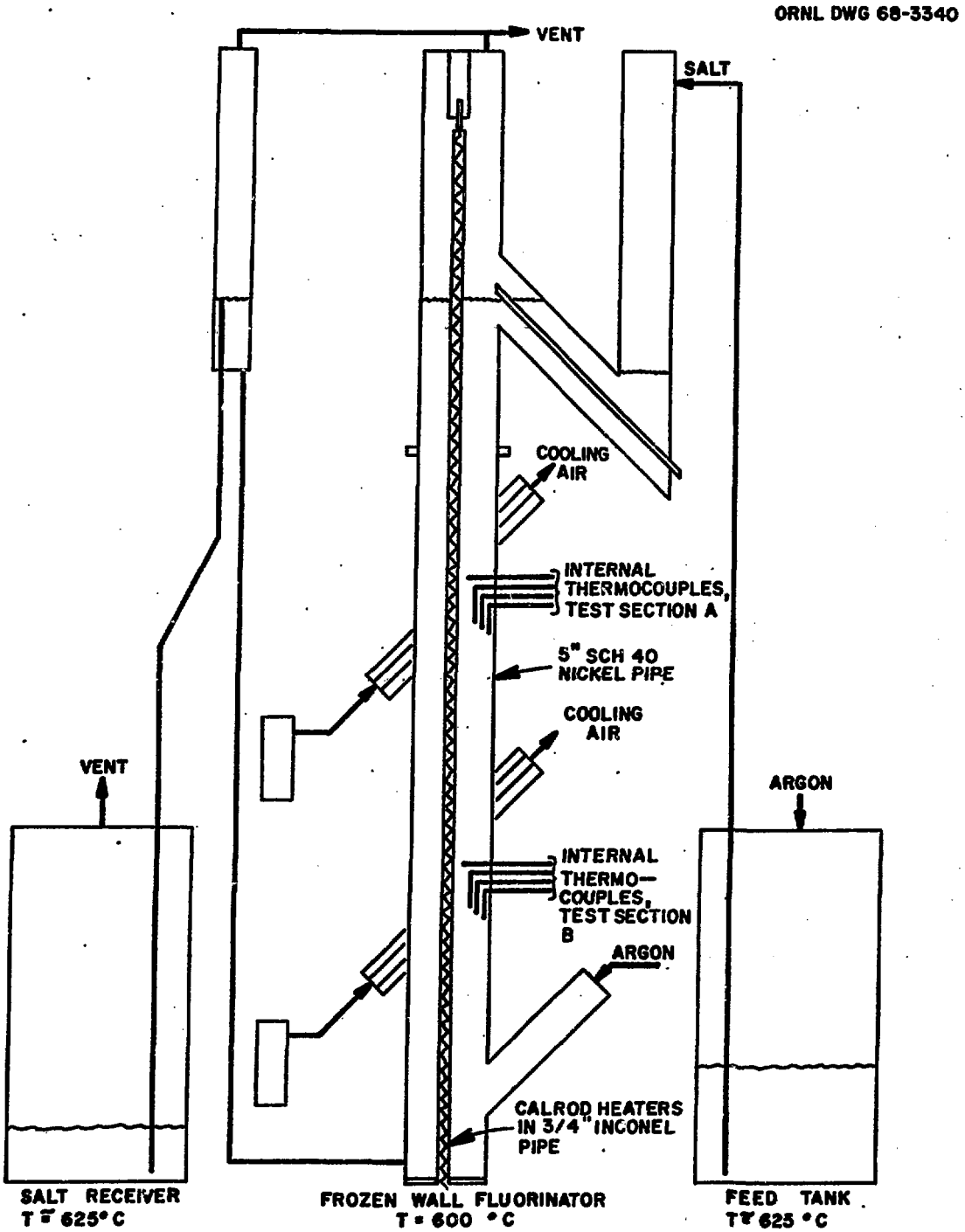

Fig. 7. Diagram of Experimental Equipment for Studying Formation of Frozen Salt Layer for Corrosion Protection.

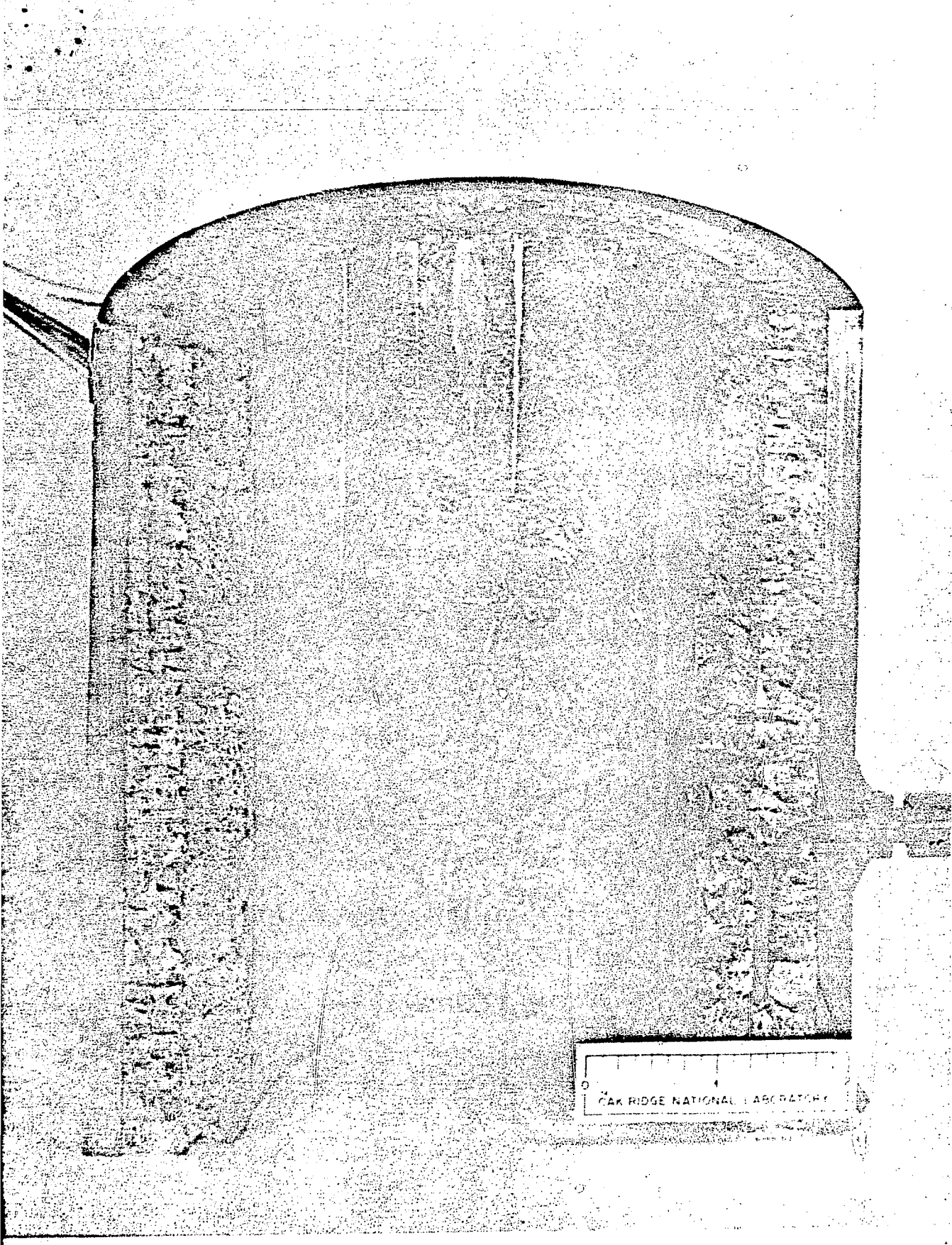

Fig. 8. Photograph of Section of Gas-Salt Contactor Showing Frozen Wall Left After Draining the Test Vessel.

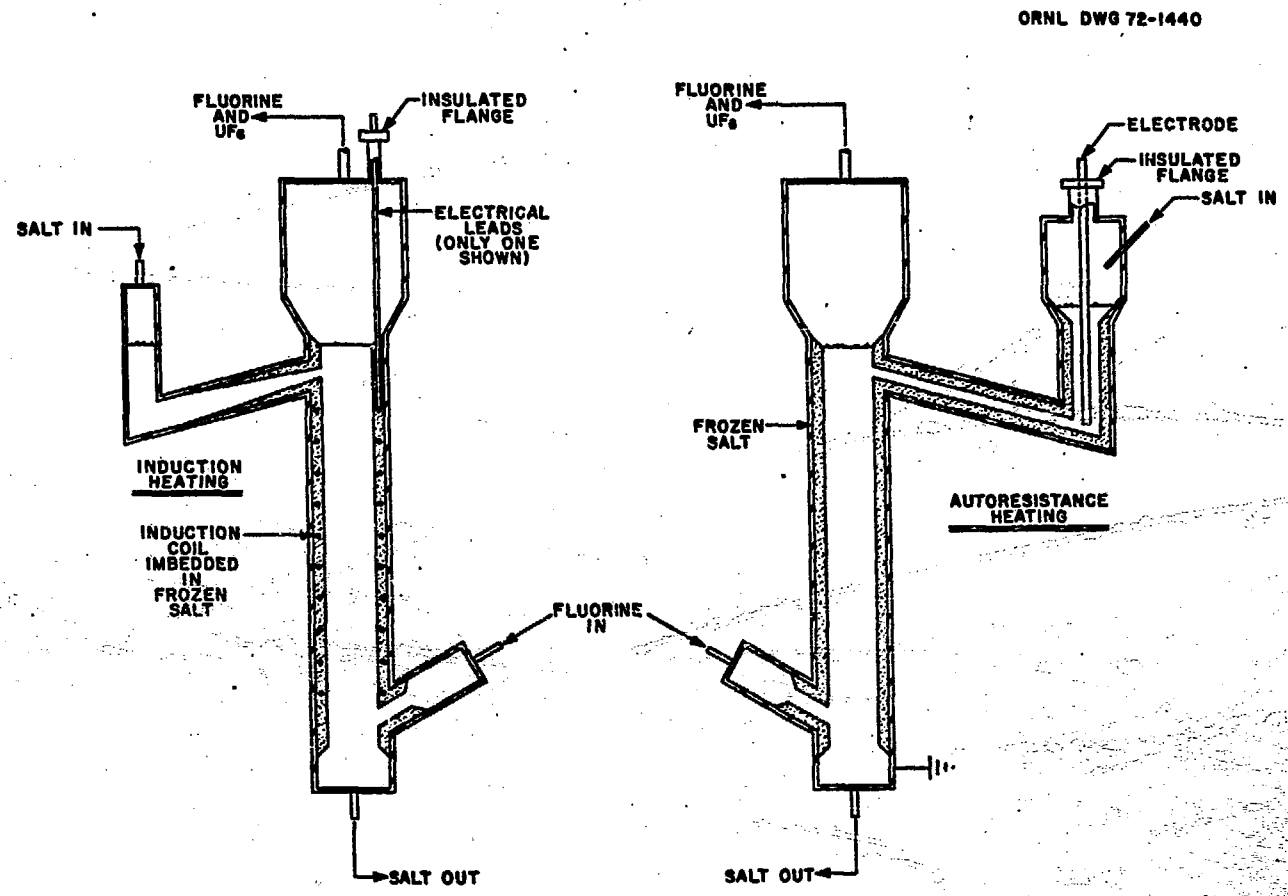

Fig. 9. Internal Heating Methods for Demonstration of Frozen Wall Corrosion Protection in a Continuous Fluorinator.

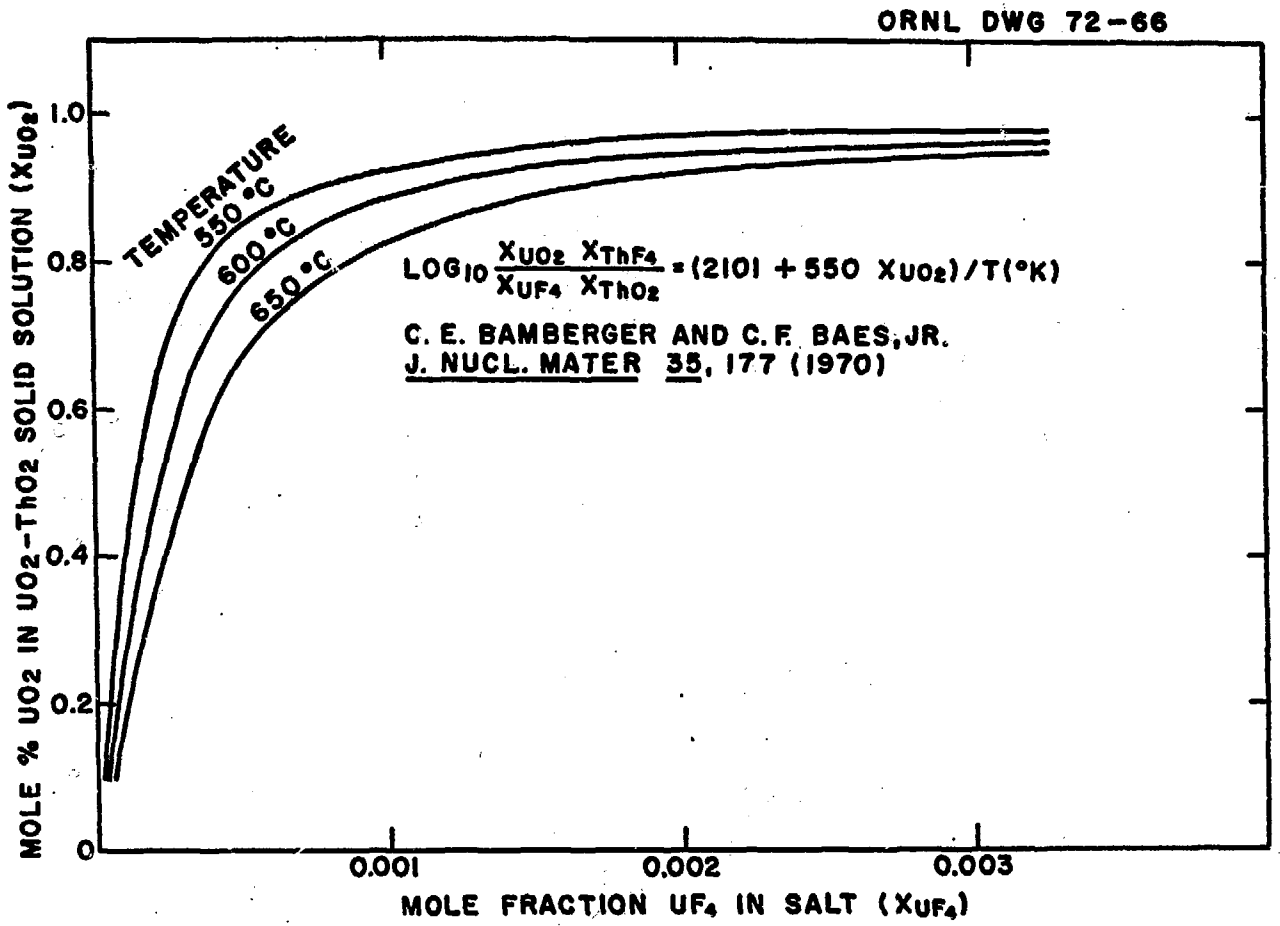

Fig. 10. Composition of UO_2-ThO_2 Solid Solution as a Function of Salt Temperature and Uranium Concentration in 72-16-12 mole % LiF-BeF_2-ThF_4 Mixture.

ORNL DWG 72-64

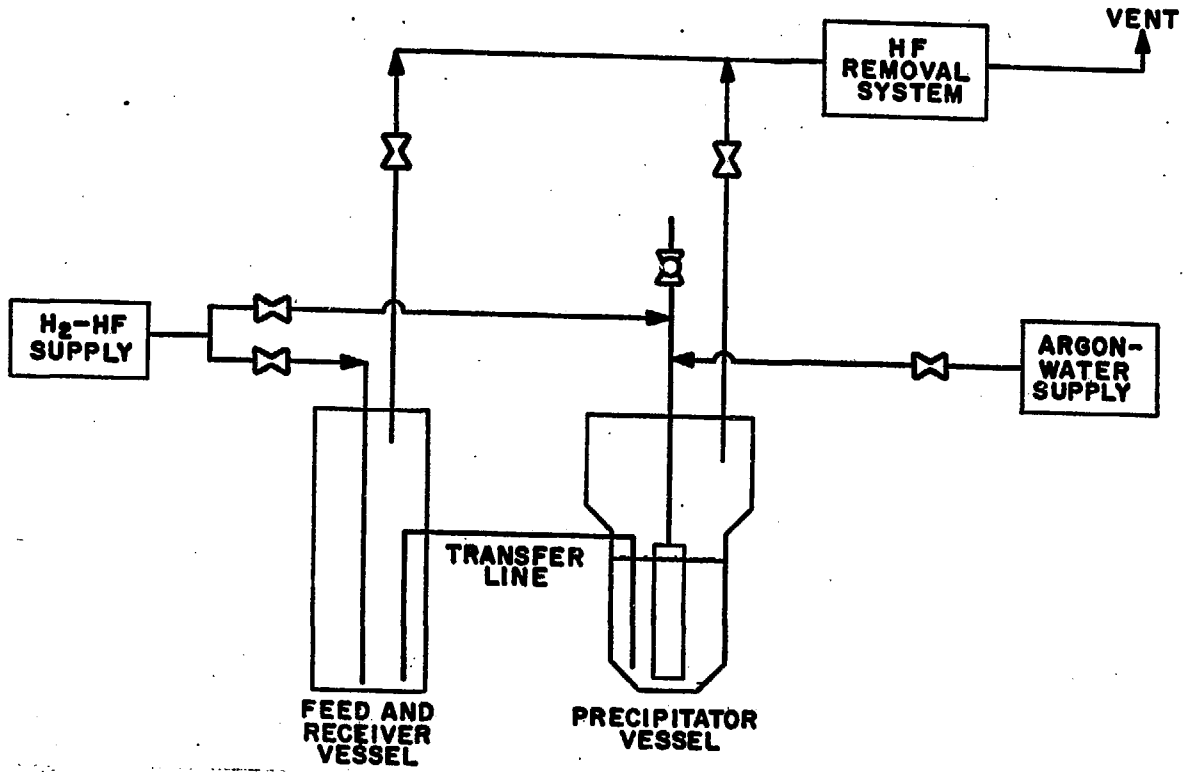

Fig. 11. Schematic Diagram for a Single Stage Oxide Precipitation Facility.

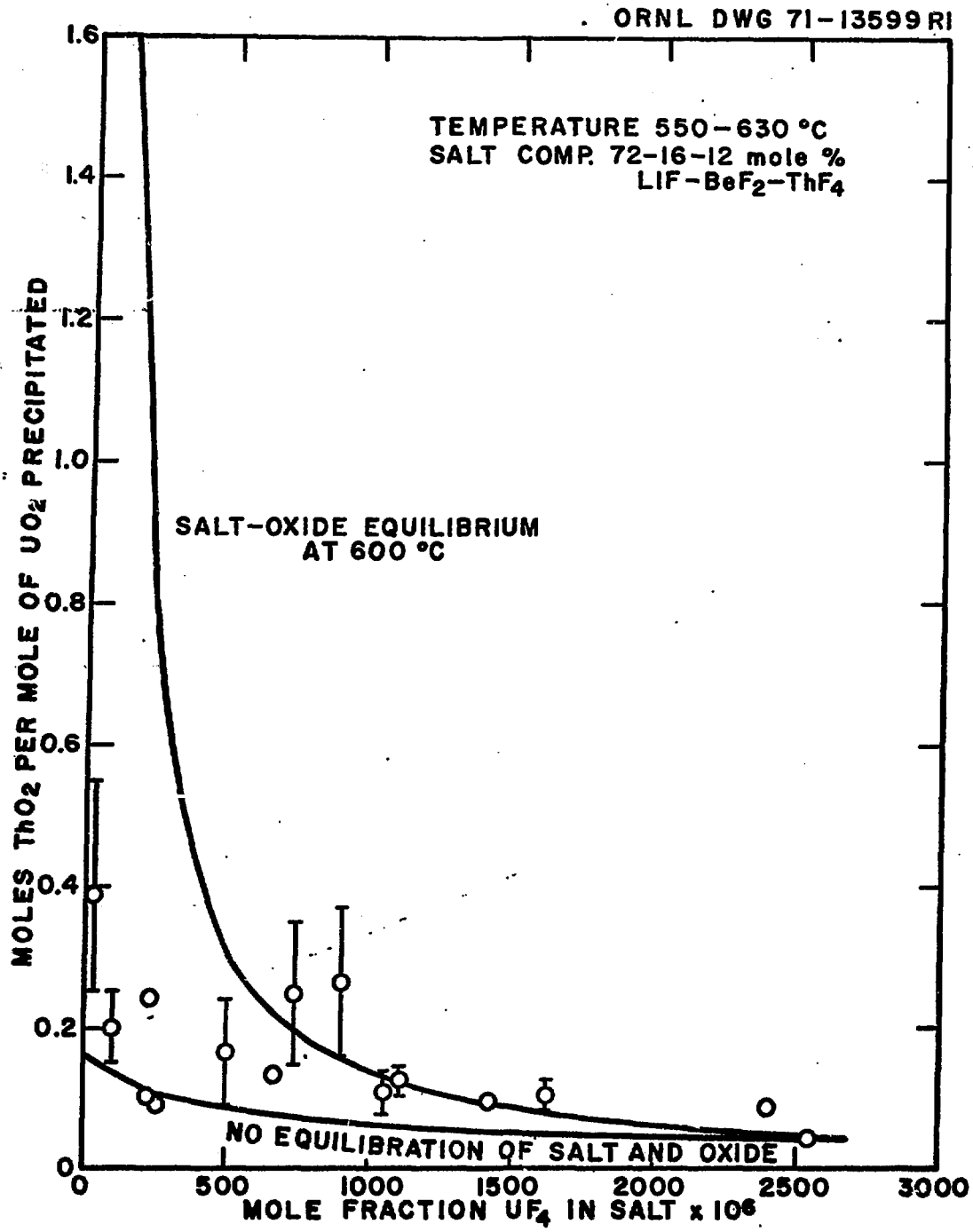

Fig. 12. Results of Oxide Analyses Taken from Oxide Precipitation Facility.